PCCP

Accepted Manuscript




ROYAL SOCIETY OF CHEMISTRY

www.rsc.org/pccp

Journal Name

ARTICLE

# Surface-functionalized monolayered nanodots of a transition metal oxide and their properties

Masashi Honda,[a] Yuya Oaki*[a] and Hiroaki Imai*[a]

Received 00th January 20xx,
Accepted 00th January 20xx

DOI: 10.1039/x0xx00000x

www.rsc.org/

Lateral size, surface chemistry, and property are varied on inorganic monolayers based on a transition metal-oxide. A variety of inorganic monolayers with their emergent properties have been studied in the recent decades. However, it is not easy to tune the lateral size, surface chemistry, and dispersibility of monolayers by typical synthetic methods. In the present work, a new approach is developed for the simultaneous surface functionalization and exfoliation of the precursor nanocrystals in a nonpolar organic medium. We obtained the monolayered nanodots of a titanium oxide less than 5 nm in the lateral size with the surface functionalization by an alkylamine ($C_{14}H_{29}NH_2$) and dihydroxynaphthalene (DHN) in toluene. The bandgap energy of the monolayers was changed by the lateral size and surface functionalization. The present study suggests versatile potentials of the monolayers with the tuned size, surface chemistry, and properties.

## Introduction,

Morphologies of nanomaterials have attracted much interest because of associations with the properties.[1–3] Monolayered nanodot, an ultrathin tiny structure, can be regarded as a new family of nanoscale morphologies. Here we have synthesized monolayered nanodots of a transition metal oxide with the functionalized surface dispersed in a nonpolar organic medium. As for nanoparticles, a variety of methods for size and morphology control have been developed in previous studies.[1] Surface chemistry of nanoparticles plays important roles for tuning of the dispersibility, assembly state, and properties.[1–4] Inorganic monolayers and their properties have been widely studied in recent years.[5,6] However, the lateral size and surface chemistry of the monolayers are not fully controlled in previous works. Our intention here is synthesis of monolayers with the tuned lateral size, surface functional group, and dispersibility. If these factors are changed, properties of the monolayers can be tuned for their wide range of applications. In the present work, the size-reduced titanate monolayers with the functionalized surface by organic molecules were obtained in a nonpolar organic medium (Fig. 1). The bandgap energies of the monolayers varied by the lateral size and surface functionalization.

In general, inorganic monolayers are synthesized by exfoliation of the precursor layered compounds in aqueous and polar organic media through introduction of bulky organic ions in the interlayer space.[5,6] However, it is not easy to tune the lateral size, surface functional group, and dispersibility of monolayers by conventional methods. The typical exfoliation methods provide the positively and negatively charged monolayers dispersed in aqueous and polar organic media. If the size of the precursor layered compounds is reduced before the delamination, the monolayers with the reduced lateral size are obtained after the exfoliation. In our previous work,[7] the monolayered nanodots of transition metal oxides were prepared from the precursor nanocrystals by the typical exfoliation method in an aqueous medium. The direct synthesis provided the size-controlled titanate monolayers around several tens nanometers in a previous report.[8] The monolayer clusters of molybdenum and tungsten sulfides and lead halides were synthesized through the direct synthetic routes.[9] However, it is not easy to prepare the monolayered nanodots with the desired functional groups and dispersibility in nonpolar organic media by the conventional exfoliation methods. A new general method for surface functionalization and dispersibility control of monolayered nanodots is required for their applications. In the present work, we adopted titanate as a model case for size reduction and surface functionalization of the monolayers.

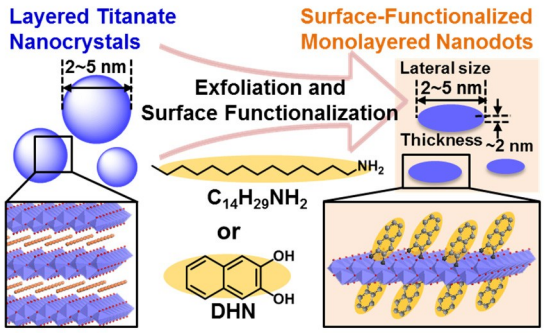


**Fig. 1** Schematic illustration for syntheses of the surface-functionalized monolayered nanodots based on titanate through simultaneous surface functionalization and exfoliation of the precursor nanocrystal.

[a] *Address here. Department of Applied Chemistry, Faculty of Science and Technology, Keio University, 3-14-1 Hiyoshi, Kohoku-ku, Yokohama 223-8522, Japan. oakiyuya@applc.keio.ac.jp, hiroaki@applc.keio.ac.jp*

† Footnotes relating to the title and/or authors should appear here.
Electronic Supplementary Information (ESI) available: [Structure analysis of the precursor layered compounds. UV-Vis spectra of e μm-$TiO_2$ and nm-$TiO_2$]. See DOI: 10.1039/x0xx00000x

In general, a variety of monolayers are synthesized and dispersed in aqueous and polar organic media. In contrast, a limited number of the surface-modified monolayers with micrometer lateral size were prepared in nonpolar organic media.[10–12] In these previous reports, organic molecules were grafted on each layer in the layered compounds. The hydrophobic interaction between the grafted organic molecules and dispersion media induced the exfoliation and dispersion of the monolayers in nonpolar organic media.[10] In these methods, however, preparation of the precursor layered composites required the multistep and long-term processes. Although the surface modification of metal-chalcogenide monolayers was reported,[12] the lateral-size variation was not achieved in the previous works. The lateral size and surface chemistry of transition-metal oxide monolayers was not changed in previous studies. Our challenge here is simultaneous exfoliation and surface functionalization of monolayers in a nonpolar organic medium. The intercalation and subsequent grafting of organic molecules facilitate the spontaneous exfoliation in nonpolar organic media based on van der Waals interaction.[10*f,g*] It is expected that the intercalation of organic molecules smoothly proceeds into the nanocrystals of the precursor layered compounds.[7,13] Therefore, a variety of surface-functionalized monolayered nanodots can be obtained through the simultaneous surface modification and exfoliation in nonpolar organic media.

In the present work, we obtained the titanate monolayered nanodots with the surface functionalization and simultaneous exfoliation by organic molecules in a nonpolar organic medium (Fig. 1). The precursor nanocrystals were synthesized through an aqueous solution process.[14] The simultaneous surface functionalization and exfoliation were achieved on the precursor nanocrystals in toluene containing organic molecules. The control of the lateral size and surface chemistry influences on the bandgap energy ($E_g$). The monolayered nanodots with the modified surface exhibit the widening of the bandgap energy ($\Delta E_g$). The surface-functionalized monolayered nanodots showed the photoexcitation of electrons from the modified organic molecules to the monolayers in visible light region. The present results show a new approach for tuning of the lateral size, surface chemistry, and properties of monolayers. In addition, the surface-functionalized monolayered nanodots with the tuned bandgap energy in visible light region have potentials for applications to visible-light responsive photocatalyst.

## Results and Discussion

### Precursor Nanocrystals of the Layered Titanate

The nanocrystals of layered sodium titanate (Na-$TiO_2$) were synthesized through the low-temperature aqueous solution route.[14] The interlayer sodium ions were exchanged to protons with immersion in hydrochloric acid (HCl). The detailed methods were described in the Experimental Section. The nanocrystals of protonated titanate (H-$TiO_2$) 2–5 nm in size were obtained in the homogeneous and disordered assembly,[14] as shown in the images of field-emission transmission electron microscopy (FETEM) (Fig. 2a). The crystal phase of the resultant titanate was assigned to the lepidocrocite-type layered titanate in our previous report.[14*a*] The Miller index was referred to the previous works.[15] The Debye-Scherrer rings corresponding to the (110) and (200) planes of the titanate were observed on the selected area electron diffraction (SAED) (the inset of Fig. 2a). The lattice fringes of the nanocrystals were assigned to the lattice spacing of the titanate on the image of high-resolution transmission electron microscopy (HRTEM) (Fig. 2b). The broadened peaks corresponding to the protonated titanate (H-$TiO_2$) were observed on the X-ray diffraction (XRD) pattern (Fig. S1 in the Electronic Supplementary Information (ESI)). In our previous work,[14*a*] the crystallite sizes were calculated to be 2.0 nm by Scherrer's equation on the XRD pattern. As a reference, the bulk H-$TiO_2$ was synthesized by solid-state reaction of cesium titanate (Cs-$TiO_2$) and the subsequent ion exchange (Fig. S1 in the ESI).[15*b*]

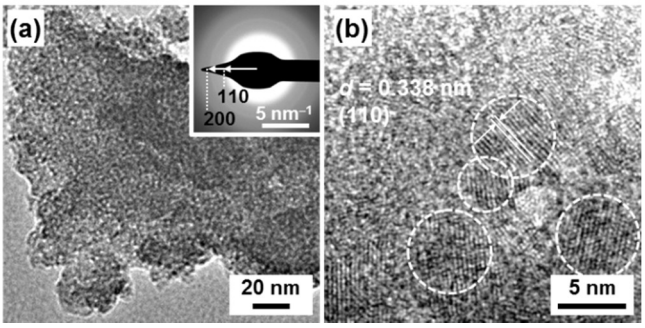


Fig. 2 Precursor nanocrystals of H-TiO2. (a) FETEM image with the SAED pattern (the inset). (b) HRTEM image.

### Formation of Surface-Functionalized Monolayered Nanodots through Simultaneous Exfoliation and Surface Modification

Tetradecylamine ($C_{14}$-$NH_2$, $C_{14}H_{29}NH_2$) and 2,3-dihydroxynaphthalene (DHN) were adopted as the organic molecules for the simultaneous surface modification and exfoliation in toluene (Fig. 1). The $C_{14}$-$NH_2$ hydrochloride electrostatically interacts with the anionic titanate layer, leading to generation of the hydrophobic surface.[10*g*] Previous reports suggest that the dihydroxy moiety of DHN coordinates the surface of titanium oxides.[16,17] The $C_{14}$-$NH_2$ and DHN-modified monolayered nanodots were obtained by the following methods. The precursor H-$TiO_2$ nanocrystals were dispersed in toluene solutions containing $C_{14}$-$NH_2$ (Fig. 1). The precursor H-$TiO_2$ nanocrystals were immersed in acetone solution of DHN for adsorption of the DHN on the particle surface. Then, these DHN-adsorbed samples were dispersed in toluene solution containing DHN. The dispersion liquids were centrifuged to remove the unexfoliated structures. The dispersion liquid of the titanate in the presence of DHN showed the orange color (the inset of Fig. 3b), whereas the dispersion liquid of the $C_{14}$-$NH_2$ modified monolayered nanodots was clear and colorless (the inset of Fig. 3a). The toluene dispersion liquids were dropped on a collodion membrane supported with copper mesh and a silicon wafer for FETEM and atomic force microscopy (AFM) observations, respectively. FETEM images

show the nanodots less than 5 nm in the lateral size (Fig. 3a,b). The same size of the white objects corresponding to the nanodots were observed on the black background in the images of high-angle-annular dark-filed scanning transmission electron microscopy (HAADF-STEM) (Fig. 3c,d).‡ Based on the HAADF-STEM images, the average lateral size was estimated to be 4.54 ± 0.50 nm (the counted sample number: $n$=33) and 4.39 ± 0.70 nm ($n$=31) for $C_{14}$-$NH_2$- and DHN-modified monolayered nanodots, respectively. The low contrast of the images imply the thin nature of the materials. The height of the nanodots was estimated to be around 1.5 nm on the AFM images with the surface modification by $C_{14}$-$NH_2$ and DHN (Fig. 3e,f).§ A small amount of the nanodots higher than 3 nm in the thickness, namely unexfoliated few-layer objects, was contained on the AFM images (Fig. 3f). The average thickness of the monolayered nanodots was estimated to be 1.23 ± 0.25 nm ($n$=8) and 1.47 ± 0.33 nm ($n$=10) for the $C_{14}$-$NH_2$- and DHN-modified ones, respectively. However, as shown in Fig. 3f, the DHN-modified titanate contained the few-layer objects with the average thickness of 2.96 ± 0.43 nm ($n$=6). In previous works, the thickness of the bare titanate monolayers was estimated to be 0.7 nm on the AFM images and structure models.[6e,6l] An increase in the height is ascribed to the grafting of $C_{14}$-$NH_2$ and DHN on the surface of the nanodots. The longitudinal axis of the DHN molecule was calculated to be approximately 0.7 nm. In contrast, the molecular length of $C_{14}$-$NH_2$ was longer than that of the DHN. The height of the $C_{14}$-$NH_2$-modified nanodots is consistent with that of the $C_{14}$-$NH_2$-modified monolayer with micrometer lateral size in our previous report.[10f] It is inferred that the alkyl chains are tilted and/or tangled on the surface of the monolayered nanodots. These results suggest that the titanate monolayered nanodots modified with $C_{14}$-$NH_2$ and DHN were obtained by the simultaneous surface modification and exfoliation in toluene.

### Bandgap Energy of the $C_{14}$-$NH_2$-Modified Monolayered Nanodots

The surface-modified monolayered nanodots show the widening of the bandgap energy originating from the size reduction and surface modification (Figs. 4 and 5). Based on our previous reports, changes of the bandgap energy are ascribed to the following two factors. The decrease in the lateral size involves an increase in the $E_g$ originating from quantum size effect, as demonstrated in our previous work[7] The surface functionalization also induces the changes of the $E_g$ because the adsorbed molecules involve the effective masses of hole and electron of the semiconductor monolayer.[10f] The $E_g$ of the $C_{14}$-$NH_2$-modified monolayered nanodots ($C_{14}$-$NH_2$/nm-$TiO_2$ monolayer) was estimated to be 4.10 eV (Fig. 4a). The $E_g$=4.10 eV is the largest value in titanium-oxide related materials, to the best of our knowledge.[18] The $\Delta E_g$ is calculated to be 0.86 eV by the difference between the bulk-size titanate (μm-$TiO_2$) and $C_{14}$-$NH_2$/nm-$TiO_2$ monolayer. The large variation of $E_g$, namely $\Delta E_g$, is ascribed to both the size reduction and surface modification as follows (Fig. 4b).

Fig. 4b summarizes the experimental $E_g$ values of the related materials.[6l,7,10f] Based on previous reports, the μm-$TiO_2$ and titanate nanocrystals (nm-$TiO_2$) 2–5 nm in size showed the $E_g$=3.24 eV and $E_g$=3.25 eV, respectively (Fig. S2 in the ESI).[10f]

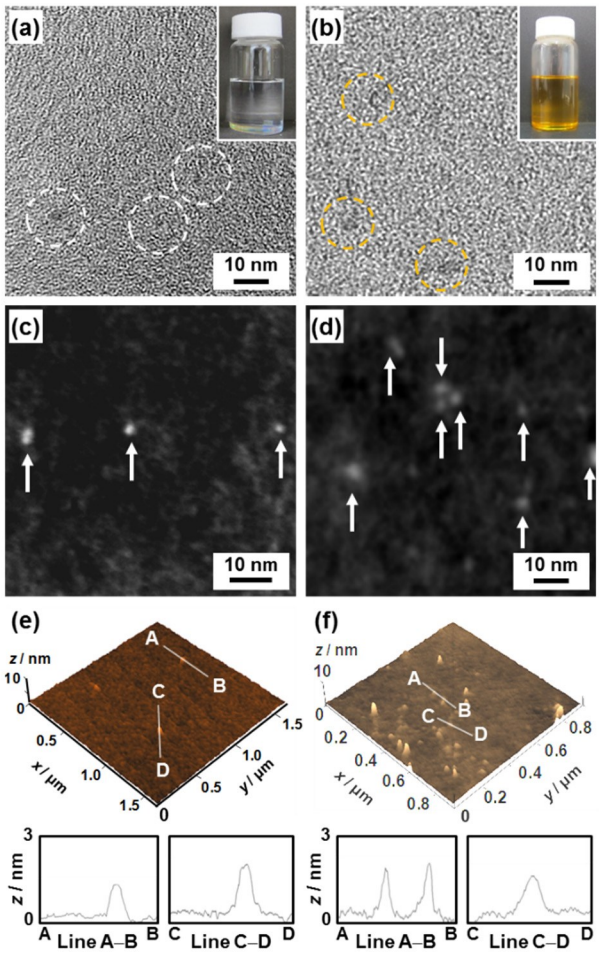


**Fig. 3** Monolayered nanodots with surface functionalization by $C_{14}$-$NH_2$ (a,c,e) and DHN (b,d,f). (a,b) bright-field FETEM images and the pictures of the dispersion liquid exhibiting light scattering with irradiation of laser light (the insets). (c,d) HAADF-STEM images showing the white dots on the black background. (e,f) AFM images and their height profiles on Si substrates.

When these precursors were exfoliated in aqueous media by the conventional methods, the $E_g$ of the μm-$TiO_2$ and nm-$TiO_2$ monolayers was estimated to be $E_g$=3.84 eV and $E_g$=3.90 eV, respectively.[6l,7] In our previous report, the $E_g$=4.06 eV was observed on the $C_{14}$-$NH_2$ modified monolayers dispersed in toluene with the micrometer lateral size ($C_{14}$-$NH_2$/μm-$TiO_2$ monolayer).[10f] In the present study, the $E_g$=4.10 eV was observed on the monolayered nanodots 2–5 nm in the lateral size modified by $C_{14}$-$NH_2$ ($C_{14}$-$NH_2$/nm-$TiO_2$ monolayer). An increase in the $E_g$, namely $\Delta E_g$=0.86 eV, is ascribed to the following two structure changes: the exfoliation with the surface modification (the arrows I–IV in Fig. 4b) and the lateral size reduction (the arrows V–VII in Fig. 4b). In general, $\Delta E_g$ of the two-dimensional planar nanostructures is described by the following equation (eq. 1),[6l,9,19]

$$\Delta E_g = \frac{h^2}{4\mu_{xy}L_{xy}^{\ 2}} + \frac{h^2}{8\mu_z L_z^{\ 2}} \quad \ldots(\text{eq. 1})$$

where $x$ and $y$ are the coordinates parallel to the plane, $z$ is the coordinate perpendicular to the plane, $L_i$ ($i$=$xy$, $z$) is the length of each coordinate, $\mu_{xy}$ and $\mu_z$ are the reduced effective masses of electron-hole pair in the corresponding coordinates, and $h$ is Planck's constant.

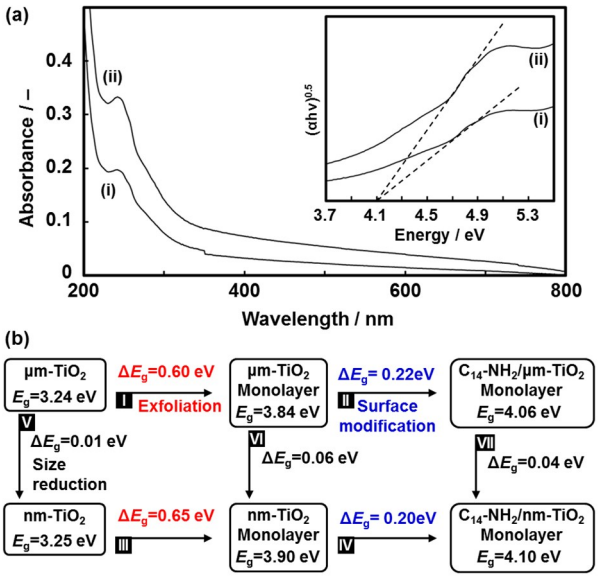


**Fig. 4** Bandgap energies of the monolayered nanodots functionalized with $C_{14}$-$NH_2$. (a) UV-Vis spectra and their Tauc's plots (the inset) of the $C_{14}$-$NH_2$ modified monolayered nanodots on a quartz glass. The dispersion liquids containing $C_{14}$-$NH_2$/nm-$TiO_2$ monolayer in toluene were dropped on the substrate. The spectra (i) and (ii) were obtained by the different numbers of the drops for the reproducibility measurements. (b) Schematic representation of the $E_g$ and $\Delta E_g$ with the exfoliation, surface modification, and lateral-size reduction. The $E_g$ of the μm-$TiO_2$ and nm-$TiO_2$ were experimental values (Fig. S2 in the ESI). The $E_g$ of the μm-$TiO_2$ monolayer,[6f,7] nm-$TiO_2$ monolayer,[7] and $C_{14}$-$NH_2$ μm-$TiO_2$ monolayer[10f] were referred to the experimental values in the previous reports.

Based on the previous works, the vertical size reduction and surface modification on the monolayers induce the changes of the reduced effective mass, such as the reduction of $\mu_z$ from 1.63$m_e$ as the value of the bulk-size titanium oxide in (eq. 1).[6l,7,10f] Since the bulk-$TiO_2$ (μm-$TiO_2$) with exfoliation and surface modification by $C_{14}$-$NH_2$, as indicated by the arrows I and II in Fig. 4b, showed $\Delta E_g$ =0.82 eV in our previous work, the reduced effective mass was calculated to be $\mu_z$=0.936$m_e$ by the (eq. 1).[10f] The nm-$TiO_2$ samples induced the $\Delta E_g$=0.85 eV, as indicated by the arrows III and IV in Fig. 4b, consistent with the $\Delta E_g$=0.82 eV of the μm-$TiO_2$ by the same structure changes with the exfoliation and surface modification by $C_{14}$–$NH_2$. The effect of the lateral size reduction is calculated to be $\Delta E_{g,calc.}$=0.019–0.12 eV by the first term of the (eq. 1) on the assumption of $L_{x,y}$= 2.0–5.0 nm and $\mu_{x,y}$=1.63$m_e$ as the reduced effective mass of bulk anatase titanium dioxide. The experimental $\Delta E_g$ values with the lateral size reduction, as indicated by the arrows V, VI, and VII in Fig. 4b, were in the range of $\Delta E_{g,calc.}$=0.019–0.12 eV on the assumption of the particle size distribution within 2–5 nm. These estimations support the $E_g$ around 4.10 eV on the surface-modified monolayered nanodots of titanate. Therefore, the combination of exfoliation, surface modification, and lateral size reduction has potentials for fine tuning of $E_g$.

**Bandgap Energy of the DHN-Modified Monolayered Nanodots**

The DHN-modified monolayered nanodots in toluene showed the changes of the absorption behavior (Fig. 5). The shift of the absorption edge to visible light region, the orange color, is ascribed to the electron excitation from the grafted DHN to the titanate monolayered nanodot (Figs. 3b and 5a). Previous reports showed the electron excitation scheme from the highest-occupied molecular orbital (HOMO) of the adsorbed organic molecules to the conduction band (CB) of metal oxides (Fig. 5a).[20] In the present work, the same excitation scheme is achieved on the titanate monolayered nanodots modified by DHN. In the present work, the energy gap between the HOMO of the organic molecules to the CB of the semiconductor monolayer is estimated from the Tauc's plot with conversion from the UV-Vis spectrum. In previous works, the calculation method was not fully developed in this type of electron transition.[21,22] The energy gap is calculated by the Tauc's plot in a couple of previous works.[21] In the other previous report,[22] the energy cap is directly calculated from the wavelength of the absorption edge. The calculation method based on the Tauc's plot was used in the present work because the calculation results were consistent with the value in our previous work. However, the further experimental and theoretical studies are required for the adequacy of the method. Here we studied the energy gap ($E_{g,HOMO\text{-}CB}$) between the HOMO level of the adsorbed DHN ($E_{HOMO}$) and the CB minimum of the titanate monolayered nanodot ($E_{CB}$) with the exfoliation and surface modification, instead of the $E_g$ between the valence band (VB) maximum ($E_{VB}$) and $E_{CB}$ (Fig. 5a). Fig. 5b,c summarizes the $E_{g,HOMO\text{-}CB}$ of the DHN-modified nanocrystal (DHN/nm-$TiO_2$) and its exfoliated monolayer (DHN/nm-$TiO_2$ monolayer). The $E_{g,HOMO\text{-}CB}$ is estimated to be 1.82 eV for the DHN/nm-$TiO_2$ (the spectrum (i) in Fig. 5b) and 2.70 eV for the DHN/nm-$TiO_2$ monolayer (the spectrum (ii) in Fig. 5b). An increase in $E_{g,HOMO\text{-}CB}$ ($\Delta E_{g,HOMO\text{-}CB}$) is ascribed to the exfoliation and surface modification because the $\Delta E_g$ induces the $\Delta E_{g,HOMO\text{-}CB}$ (Fig. 5a). A previous report suggested that the $E_{HOMO}$ of the adsorbed organic molecules is pinned on the Fermi level ($E_F$) of semiconductor metal oxides, namely $E_{HOMO}$=$E_F$.[23] The $E_F$ is shifted with the changes of $E_{VB}$ originating from the quantum-size effect.[24] Based on these facts, the $\Delta E_g$ is assumed to be equal to $\Delta E_{g,HOMO\text{-}CB}$, namely $\Delta E_g$=$\Delta E_{g,HOMO\text{-}CB}$ (Fig. 5a). Therefore, the calculation study by using the (eq. 1) is applied to $\Delta E_{g,HOMO\text{-}CB}$ as well as $\Delta E_g$. In the present work, the exfoliation of the DHN/nm-$TiO_2$ into the monolayers induced the $\Delta E_{g,HOMO\text{-}CB}$=0.88 eV (Fig. 5a). The $\Delta E_{g,HOMO\text{-}CB}$ of 0.88 eV was slightly different from the $\Delta E_g$=0.82 eV of the μm-$TiO_2$, as indicated by the arrows I and II in Fig. 2b. The slight differences are attributed to those of the hypotheses, such as the assumptions of $\Delta E_{g,HOMO\text{-}CB}$=$\Delta E_g$ and the reduced effective mass ($\mu_z$=0.936$m_e$). If the $\mu_z$ is assumed to be the smaller value for the DHN-modified monolayers, the calculated $\Delta E_g$ is consistent with the experimental $\Delta E_{g,HOMO\text{-}CB}$. These results suggest that bandgap energy of the monolayers, such as $E_g$ and $E_{g,HOMO\text{-}CB}$, can be tuned by the variation of the lateral size and surface chemistry.

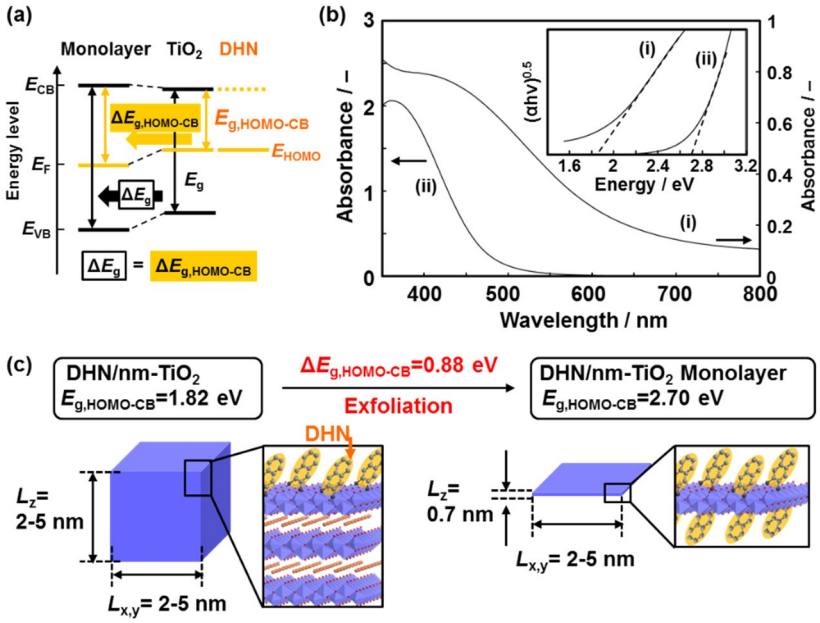


**Fig. 5** Bandgap energies of the monolayered nanodots functionalized with DHN. a) Schematic energy diagram of the monolayer, precursor layered titanate, and DHN. b) UV-Vis spectra and their Tauc's plots of the DHN/nm-$TiO_2$ (i) and DHN/nm-$TiO_2$ monolayer (ii). (e) Schematic representation for the $E_{g,HOMO-CB}$ and $\Delta E_{g,HOMO-CB}$ of the DHN/nm-$TiO_2$ and its exfoliated DHN/nm-$TiO_2$ monolayer.

## Conclusions

The lateral size and surface chemistry were changed on the monolayer of a transition metal oxide. The monolayered nanodots of titanate less than 5 nm in the lateral size with the surface functionalization by $C_{14}$-$NH_2$ and DHN were obtained in a nonpolar organic medium. The nanocrystals of the layered titanate were used as the precursor. The precursor nanocrystals were dispersed in toluene containing $C_{14}$-$NH_2$ and DHN. The surface-modified monolayered nanodots were obtained by the simultaneous exfoliation and surface functionalization. The present methods can be applied to the other combinations of the layered compounds and surface modifiers. The resultant monolayered nanodots with the surface modification by $C_{14}$-$NH_2$ and DHN showed the tuned bandgap energies. The results imply that bandgap engineering of monolayers can be achieved by the control of the lateral size and surface chemistry. Tuning of lateral size and surface chemistry has potentials for development of functional monolayered materials with the tuned properties. Furthermore, surface-functionalized monolayered nanodots with the tuned bandgap energy in visible light region have potentials for applications to visible-light responsive photocatalyst. The variation of $E_{CB}$ on the monolayered nanodots induces the enhancement of the oxidation potency.

## Experimental Section

All the reagents were used without purification. Purified water was used for all the experiments.

### Synthesis of the Precursors

The nanocrystals of layered sodium titanate (Na-$TiO_2$) were synthesized by the method in our previous reports.[19a] An aqueous solution containing 5 mmol $dm^{-3}$ titanium fluoride ($TiF_4$, Aldrich) was mixed with an equal volume of 50 mmol $dm^{-3}$ sodium hydroxide (NaOH, Junsei 97.0 %) aqueous solution at room temperature. The sample bottle was maintained without stirring at 25 ˚C for 3 days. The precipitates were centrifuged and then dried at room temperature. Then, 1.0 g of the resultant Na-$TiO_2$ nanocrystal was immersed in 100 $cm^3$ of 1 mol $dm^{-3}$ hydrochloric acid (HCl) aqueous solution for 3 days at 25 ˚C. The nanocrystals of the protonated titanate (H-$TiO_2$) were obtained after the centrifugation and drying. The bulk-size crystals of cesium titanate (Cs-$TiO_2$) were synthesized by a solid-state reaction reported in a previous paper.[20] The mixture of rutile titanium dioxide ($TiO_2$, Junsei, 99%) and cesium carbonate ($CsCO_3$, Junsei, 99%) were calcined at 800 ˚C for 20 h in air. The interlayer cesium ion was exchanged to proton by the same procedure as mentioned above.

### Surface functionalization and exfoliation of the precursor nanocrystals

The surface functionalization and exfoliation of the precursors were performed by tetradecylamine ($C_{14}H_{29}NH_2$, $C_{14}$-$NH_2$, Tokyo Kasei, 95%) and 2,3-dihydroxynaphthalene (DHN, Tokyo Kasei, 97%) in toluene medium. As for $C_{14}$-$NH_2$, 0.05 g of the H-$TiO_2$ nanocrystals (nm-$TiO_2$) and bulk-size H-$TiO_2$ (μm-$TiO_2$) were immersed in 20 $cm^3$ of the toluene solution containing 0.01 g of

$C_{14}$-$NH_2$ for 5 days at 60 ˚C. The resultant dispersion liquids were centrifuged at 13500 rpm for 10 min to remove the unexfoliated materials as the precipitates. As for DHN, 0.07 g of the nm-$TiO_2$ was immersed in 7 $cm^3$ acetone solution containing 1.5 g of DHN prior to the exfoliation. After the washing by acetone, the DHN-adsorbed titanate sample, namely DHN/nm-$TiO_2$, was centrifuged and then collected. Then, 0.025 g of the DHN/nm-$TiO_2$ sample was dispersed in 20 $cm^3$ toluene solution containing 0.005 g of DHN for 5 days at 60 ˚C to induce the exfoliation and surface modification. The resultant dispersion liquids were centrifuged at 13500 rpm for 10 min to remove the unexfoliated materials.

### Characterization

The morphologies and the lateral sizes of the resultant materials were observed by using a field-emission transmission electron microscopy (FETEM, Tecnai G2) operated at 200 kV. The height of the monolayered structures was measured by atomic force microscopy (AFM, Shimadzu SPM-9600). The dispersion liquids of the monolayered nanodots were dropped on a collodion membrane supported by copper grids and on a cleaned silicon substrate for FETEM and AFM observations, respectively. The bandgap energies were estimated from the UV-Vis absorption spectra (UV-Vis, JASCO V-670). The UV-Vis spectra of the precursor layered structures were obtained by the diffuse-reflectance spectroscopy of the powders. The powder of magnesium oxide was used as the reference. The dispersion liquid of $C_{14}$-$NH_2$/nm-$TiO_2$ monolayers was condensed by the evaporation of toluene. The concentrated dispersion liquid was dropped typically by ca. 0.02 $cm^3$ for ~10 times on a quartz glass substrate set on a heating stage at 50 ˚C. In this case, a quartz glass substrate was used as the reference. The dispersion liquids of the DHN-modified samples were poured into the quartz glass cell. These samples were measured by a transmittance mode.

## Acknowledgements

This work was partially supported by Grant-in-Aid for Scientific Research (No. 22107010) on Innovative Areas of “Fusion Materials: Creative Development of Materials and Exploration of Their Function through Molecular Control” (No. 2206) (H.I.) from the MEXT and Challenging Exploratory Research (No. 24655199) (Y.O.) from JSPS.

## Notes and references

‡ The low-contrast cloudy objects except the arrowed ones were observed on the background of the HAADF-STEM images. These objects were caused by the deposition of the $C_{14}$-$NH_2$ and DHN dissolved in toluene. In the present method, an excess amount of these surface modifiers were contained in the dispersion liquid.

§ The lateral length scale of the AFM observation generally depends on the curvature factor of a cantilever originating from the factory-default value and the deterioration with the use. Therefore, we concluded that the correct lateral sizes of the monolayered nanodots were not estimated from the AFM observations. In the present study, the thickness and the lateral size were estimated from the AFM observation and the TEM images, respectively. These characterization techniques were established in our previous works.[7,10f]

1 (*a*) Y. Yin and A. P. Alivisatos, *Nature*, 2005, **473**, 664; (*b*) J. Park, J. Joo, S. C. Kwon, Y. Jang and T. Hyeon, *Angew. Chem. Int. Ed*., 2007, **46**, 4630; (*c*) N. Pinna and M. Niederberger, *Angew. Chem. Int. Ed.*, 2008, **47**, 5292; (*d*) W. T. Yao and S. H. Yu, *Adv. Funct. Mater.*, 2008, **18**, 3357; (*e*) K. Ramasamy, M. A. Malik, N. Revaprasadu and P. O’Brien, *Chem. Mater.*, 2013, **25**, 3551; (*f*) H. C. Zeng, *Acc. Chem. Res.*, 2013, **46**, 226.

2 (*a*) H. Cölfen and M. Antonietti, *Angew. Chem. Int. Ed.*, 2005, **44**, 5576; (*b*) M. Niederberger and H. Cölfen, *Phys. Chem. Phys. Chem.* 2006, **8**, 3271; (*c*) L. Zhou and P. O’Brien, *Small*, 2008, **4**, 1566; (*d*) L. Zhou and P. O’Brien, *J. Phys. Chem. Lett.*, 2012, **3**, 620.

3 (*a*) H. Imai and Y. Oaki, *MRS Bull.*, 2010, **35**, 138; (*b*) Y. Oaki and H. Imai, *Angew. Chem. Int. Ed.*, 2005, **44**, 6571; (*c*) Y. Oaki and H. Imai, *Adv. Funct. Mater.*, 2005, **15**, 1407.

4 (*a*) C. H. Cui and S. H. Yu, *Acc. Chem. Res.*, 2013, **46**, 1427; (*b*) R. Mout, D. F. Moyano, S. Rana and V. M. Rotello, *Chem. Soc. Rev.*, 2012, **41**, 2539.

5 (*a*) R. E. Schaak and T. E. Mallouk, *Chem. Mater.*, 2002, **14**, 1455; (*b*) R. Ma and T. Sasaki, *Adv. Mater.*, 2010, **22**, 5082; (*c*) H. Okamoto, Y. Sugiyama and H. Nakano, *Chem. Eur. J.*, 2011, **17**, 9864; (*d*) T. Nakato and N. Miyamoto, *Materials*, 2009, **2**, 1734. (*e*) Q. Wang and D. O’Hare, *Chem. Rev.*, 2012, **112**, 4124; (*f*) V. Nicolosi, M. Chhowalla, M. G. Kanatzidis, M. S. Strano and J. N. Coleman, *Science*, 2013, **340**, 1226419; (*g*) M. Osada and T. Sasaki, *Adv. Mater.*, 2012, **24**, 210.

6 (*a*) A. Lerf and R. Schöllhorn, *Inorg. Chem.*, 1977, **16**, 2950; (*b*) L. F. Nazar and A. J. Jacobson, *J. Chem. Soc. Chem. Commun.*, 1986, 570; (*c*) K. Domen, Y. Ebina, S. Ikeda, A. Tanaka J. N. Kondo and K. Maruya, *Catal. Today*, 1996, **28**, 167. (*d*) T. Sasaki, M. Watanabe, H. Hashizume, H. Yamada and H. Nakazawa, *J. Am. Chem. Soc.*, 1996, **118**, 8329. (*e*) T. Sasaki and M. Watanabe, *J. Am. Chem. Soc.*, 1998, **120**, 4682; (*f*) R. E. Schaak and T. E. Mallouk, *Chem. Mater.*, 2000, **12**, 3427; (*g*) M. Adachi-Pagano, C. Forano and J. P. Besse, *Chem. Commun.*, 2000, 91; (*h*) T. Hibino and J. Willam, *J. Mater. Chem.*, 2001, **11**, 1321; (*i*) N. Yamamoto, T. Okuhara and T. Nakato, *J. Mater. Chem.*, 2001, **11**, 1858; (*j*) N. Miyamoto, H. Yamamoto, R. Kaito and K. Kuroda, *Chem. Commun*., 2002, 2378; (*k*) R. E. Schaak and T. E. Mallouk, *Chem. Commun*., 2002, 706; (*l*) N. Sakai, Y. Ebina, K. Takada and T. Sasaki, *J. Am. Chem. Soc.*, 2004, **126**, 5851; (*m*) N. Sakai, K. Fukuda, Y. Omomo, Y. Ebina, K. Takada and T. Sasaki, *J. Phys. Chem. C*, 2008, **112**, 5197; (*n*) H. B. Yao, L. H. Wu, C.H. Cui, H. Y. Fang and S. H. Yu, *J. Mater. Chem.*, 2010, **20**, 5190; (*o*) H. B. Yao, L. B. Mao, Y. X. Yan, H. P. Cong, X. Lei, S. H. Yu, *ACS Nano*, 2012, **6**, 8250; (*p*) Y. Kuroda, K. Ito, K. Itabashi and K. Kuroda, *Langmuir*, 2011, **27**, 2028.

7 K. Nakamura, Y. Oaki and H. Imai, *J. Am. Chem. Soc.*, 2013, **135**, 4501.

8 E. L. Tae, K. E. Lee, J. S. Jeong and K. B. Yoon, *J. Am. Chem. Soc.*, 2008, **130**, 6534.

9 (*a*) C. J. Sandroff, S. P. Kelty and D. M. Hwang, *J. Chem. Phys.*, 1986, **85**, 5337; (*b*) O. I. Micic, L. Zongguan, G. Mills. J. C. Sullivan and D. Meisel, *J. Phys. Chem.*, 1987, **91**, 6221.

10 (*a*) A. Usuki, Y. Kojima, M. Kawasumi, A. Okada, Y. Fukushima, T. Kurauchi and O. Kamigaito, *J. Mater. Res.*, 1993, **8**, 1179; (*b*) S. Tahara, Y. Takeda and Y. Sugahara, *Chem. Mater.*, 2005**, 17**, 6198; (*c*) H. Nakano, M. Nakano, K. Nakanishi, D. Tanaka, Y. Sugiyama, T. Ikuno, H. Okamoto and T. Ohta, *J. Am. Chem. Soc.*, 2012, **134**, 5452; (*d*) V. V. Naik, T. N. Ramesh and S. Vsudevan, *J. Phys. Chem. Lett.*, 2011, **2**, 1193; (*e*) S. Osada, A. Iribe and K. Kuroda, *Chem. Lett.*, 2013, **42**, 80. (*f*) M. Honda, Y. Oaki and H.

Imai, *Chem. Mater.*, 2014, **26**, 3579. (*g*) M. Honda, Y. Oaki and H. Imai, *Chem. Commun.*, 2015, **51**, 10446.

11 (*a*) G. Hu, N. Wang, D. O'Hare and J. Davis, *Chem. Commun.*, 2006, 287; (*b*) C. Altavilla, M. Sarno and P. Ciambelli, *Chem. Mater.*, 2011, **23**, 3879;

12 (*a*) Y. Guo, K. Xu, C. Wu, J. Zhao and Y. Xie, *Chem. Soc. Rev.*, 2015, **44**, 637; (*b*) C. Lin, X. Zhu, J. Feng, C. Wu, S. Hu, J. Peng, Y. Guo, L. Peng, J. Zhao, J. Huang, J. Yang and Y. Xie, *J. Am. Chem. Soc.*, 2013, **135**, 5144.

13 Y. Kuroda, Y. Miyamoto, M. Hibino, K. Yamaguchi and N. Mizuno, *Chem. Mater.*, 2013, **25**, 2291.

14 (*a*) Y. Oaki, K. Nakamura and H. Imai, *Chem. Eur. J.*, 2012, **18**, 2825; (*b*) Y. Oaki, T. Anzai and H. Imai, *Adv. Funct. Mater.*, 2010, **20**, 4127.

15 (*a*) R. Ma, K. Fukuda, T. Sasaki, M. Osada and Y. Bando, *J. Phys. Chem. B*, 2005, **109**, 6210; (*b*) T. Sasaki, Y. Komatsu and Y. Fujiki, *J. Chem. Soc., Chem. Commun.*, 1991, 817.

16 Q. Ye, F. Zhou and W. Liu, *Chem. Soc. Rev.*, 2011, **40**, 4244.

17 T. Kamegawa, H. Seto, S. Matsuura and H. Yamashita, *ACS Appl. Mater. Interface*, 2012, **4**, 6635.

18 (*a*) N. Satoh, T. Nakahima, K. Kamikura and K. Yamamoto, *Nat. Nanotech.*, 2008, **3**, 106; The nanoparticles with $E_g$=3.89 eV were prepared by using the dendrimter as the template. (*b*) Lamberti, C. *Micropor. Mesopor. Mater.*, 1999, **30**, 155. The quantum wires consisting of –Ti–O–Ti– with $E_g$=4.03 eV were embedded in the silica-based matrices. In ref. 15, the $C_{14}$-$NH_2$–modified titanate monolayers with the micrometer lateral size showed $E_g$=4.06 eV.

19 L. Kavan, T. Stoto and M. Grätzel, *J. Phys. Chem.,* 1993, **97**, 9493.

20 (*a*) J. Moser, S. Punchihewa, P. P. Infelta and M. Grätzel, *Langmuir*, 1991, **7**, 3012; (*b*) P. Persson, R. Bergström and S. Lunell, *J. Phys. Chem. B*, 2000, **104**, 10348; (*c*) E. L. Tae, S. H. Lee, J. K. Lee, S. S. Yoo, E. J. Kang and K. B. Yoon, *J. Phys. Chem. B*, 2005, **109**, 22513.

21 (*a*) J. M. Notestein, E. Iglesia and A. Katz, *Chem. Mater.*, 2007, **19**, 4998. (*b*) S. Higashimoto, T. Nishi, M. Yasukawa, M. Azuma, Y. Sakata and H. Kobayashi, *J. Catal.*, 2015, **329**, 286.

22 T. D. Savić, I. A. Janković, Z. V. Šaponjić, M. I. Čomor, D. Ž. Velijković, S. D. Zarić and J. M. Nedeljković, *Nanoscale*, 2012, **4**, 1612.

23 M. T. Greiner, M. G. Helander, W. M. Tang, Z. B. Wang, J. Qiu and Z. H. Lu, *Nat. Mater.*, 2012, **11**, 76.

24 X. Axnanda, M. Scheele, E. Crumlin, B. Mao, R. Chang, S. Rani, M. Faiz, S. Wang, A. P. Alivisatos and Z. Liu, *Nano Lett.*, 2013, **13**, 6176.